Check for updates

AGU100 ADVANCING EARTH AND SPACE SCIENCE

Geophysical Research Letters

RESEARCH LETTER
10.1029/2019GL086381

Atmospheric ^{81}Kr as an Integrator of Cosmic-Ray Flux on the Hundred-Thousand-Year Time Scale

J. C. Zappala[1], D. Baggenstos[2], C. Gerber[2,3], W. Jiang[1,4], B. M. Kennedy[5], Z.-T. Lu[1,4], J. Masarik[6], P. Mueller[1], R. Purtschert[2], and A. Visser[7]

[1]Physics Division, Argonne National Laboratory, Lemont, IL, USA, [2]Climate and Environmental Physics, Physics Institute and Oeschger Centre for Climate Change Research, University of Bern, Bern, Switzerland, [3]CSIRO Land and Water, Glen Osmond, Southern Australia, Australia, [4]Hefei National Laboratory for Physical Sciences at the Microscale, CAS Center for Excellence in Quantum Information and Quantum Physics, University of Science and Technology of China, Hefei, China, [5]Earth Sciences Division, Lawrence Berkeley National Laboratory, Berkeley, CA, USA, [6]Department of Nuclear Physics, Comenius University, Bratislava, Slovakia, [7]Nuclear and Chemical Sciences Division, Lawrence Livermore National Laboratory, Livermore, CA, USA

Key Points:
- Conducted new precision measurement of ^{81}Kr isotopic abundance in the atmosphere; new result differs significantly from previous values
- First ever cosmic-ray flux models of ^{81}Kr production in the atmosphere are presented; models successfully predict new measured value
- Measurement and models provide more accurate input function for radiokrypton dating over the past 1.5 Myr

Supporting Information:
- Supporting Information S1
- Figure S1

Correspondence to:
J. C. Zappala, and Z.-T. Lu,
jzappala@anl.gov;
ztlu@ustc.edu.cn

Citation:
Zappala, J. C., Baggenstos, D., Gerber, C., Jiang, W., Kennedy, B. M., Lu, Z.-T., et al. (2020). Atmospheric ^{81}Kr as an integrator of cosmic-ray flux on the hundred-thousand-year time scale. *Geophysical Research Letters*, *47*, e2019GL086381. https://doi.org/10.1029/2019GL086381

Received 22 NOV 2019
Accepted 10 JAN 2020
Accepted article online 21 JAN 2020
Published online 16 FEB 2020

©2020. American Geophysical Union. All Rights Reserved. This article has been contributed to by US Government employees and their work is in the public domain in the USA.

source: https://doi.org/10.48350/158635 | downloaded: 12.10.2024

Abstract The atmospheric abundance of ^{81}Kr is a global integrator of cosmic rays. It is insensitive to climate shifts, geographical variations, and short-term solar cycle activity, making it an ideal standard to test models of cosmic-ray flux on the time scale of 10^5 years. Here we present the first calculation of absolute ^{81}Kr production rates in the atmosphere, and a measurement of the atmospheric ^{81}Kr/Kr abundance via the Atom Trap Trace Analysis method. The measurement result significantly deviates from previously reported values. The agreement between measurement and model prediction supports the current understanding of the production mechanisms. Additionally, the calculated ^{81}Kr atmospheric inventory over the past 1.5 Myr provides a more accurate input function for radiokrypton dating.

Plain Language Summary Krypton-81 is a long-lived radioactive isotope produced in the Earth's atmosphere by cosmic rays. It stays in the atmosphere as a noble gas for hundreds of thousands of years until its eventual nuclear decay. As a result, its abundance uniquely reflects the long-term accumulation record of cosmic rays across the entire globe. We performed the first precise measurement of the atmospheric abundance of krypton-81. The result agrees with the prediction of a realistic isotope production model, thus confirming the current understanding of the cosmic-ray flux, isotope production mechanisms, and the past terrestrial and space magnetic field environment.

1. Introduction

Long-lived cosmogenic radionuclides are messengers carrying information about the past terrestrial and space environments (Beer et al., 2011). The ^{10}Be (half-life = 1.4 Myr), for example, effectively records the flux of cosmic rays entering the Earth's atmosphere, particularly of the galactic cosmic-ray (GCR) component, over the past 10^5–10^6 years (Beer et al., 2013). The variation of the flux in space and time is revealed by the ^{10}Be concentrations in polar ice (Finkel & Nishiizumi, 1997) and sea sediments (Carcaillet et al., 2003; Frank et al., 1997). Variation as large as 40% was found in correlation with the changing magnetic fields in the heliosphere, which follows the Schwabe (11-year) and other short-term cycles (Beer et al., 1990; McCracken et al., 2002). This solar modulation effect agrees with modern real-time neutron flux measurements in the atmosphere (Usoskin & Kovaltsov, 2008). On a longer time scale, the flux is affected by the changing magnetic fields of the Earth, an effect that has been demonstrated by comparing ^{10}Be with the geomagnetic fields, both recorded in sediments (Carcaillet et al., 2003; Frank et al., 1997). A similar effect of geomagnetic modulation within the past 100 kyr has also been observed using ^{36}Cl (half-life = 301 kyr; Baumgartner et al., 1998). Considering a plausible link between the cosmic-ray flux and cloud formation or solar irradiance, the long-term flux record derived from the ^{10}Be measurements has assisted in paleoclimate discussions (Bard & Frank, 2006; Sharma, 2002).

The ^{81}Kr (half-life = 229 ± 11 kyr; Baglin, 2008) in the atmosphere is also cosmogenic in origin and records the GCR flux on the time scale of 10^5 years. ^{81}Kr provides a complementary perspective to that of ^{10}Be (or ^{36}Cl) because of differences in their transport and residence properties in the atmosphere. ^{10}Be stays in the atmosphere for typically a few years or less. Its rate of deposition on the ground, affected by both the

distribution of cosmic-ray flux and atmospheric transport factors, varies with time and position over the globe by as much as a factor of 10 (Beer et al., 2013). As a result, understanding its transport process using large, sophisticated climate models is a critical step in the analysis of the cosmic-ray flux (Heikkila et al., 2013). In contrast, ^{81}Kr is a noble-gas nuclide and predominantly stays in the atmosphere throughout its long lifetime. Consequently, the ^{81}Kr/Kr ratio is completely insensitive to the solar cycles that act over short time scales. Only ~2% of the total terrestrial Kr content is absorbed into the oceans (Ozima & Podosek, 2001), and anthropogenic ^{81}Kr is less than 1% of the total atmospheric ^{81}Kr inventory, as verified by measurements in this work. The tracer is also mixed in the atmosphere over time scales of one to two years, and thus free of geographical variations. In summary, the ^{81}Kr/Kr ratio in the atmosphere is the ideal whole-Earth integrator of the cosmic-ray flux on the time scale of 10^5 years. Due to this simplicity, the measured ^{81}Kr/Kr value can serve as a proving ground for models that simulate cosmic-ray fluxes and calculate the production rates of cosmogenic nuclides. Here we report on the first calculation of the production rates of ^{81}Kr in the Earth's atmosphere as well as a precision measurement of the ^{81}Kr/Kr ratio in the atmosphere using the Atom Trap Trace Analysis (ATTA) method (Chen et al., 1999), the result of which differs significantly from all previously reported values.

2. Model for the Production of ^{81}Kr

The interactions of cosmic-ray particles with the atmosphere produce a cascade of secondary particles. Models have been developed to simulate these processes and calculate the production rates of cosmogenic nuclides (Beer et al., 2013; Masarik & Beer, 1999; Webber & Higbie, 2003). The production rate of ^{81}Kr at the atmospheric position D can be calculated as

$$P(D,M,\Phi) = \sum_i N_i \sum_k \int_0^\infty \sigma_{ik}(E_k) \cdot J_k(E_k,D,M,\Phi) \mathrm{d}E_k \tag{1}$$

Here N_i is the number of atoms for target element i per kg material in the atmospheric sample, σ_{ik} (E_k) is the cross section for the production of ^{81}Kr from the target element i by particles of type k with energy E_k, and J_k (E_k,D,M,Φ) is the total flux of particles of type k with energy E_k at location D within the atmosphere for the geomagnetic field M and the solar modulation parameter Φ. In this model, the particle fluxes J_k (E_k,D,M,Φ) are calculated by interfacing the GEANT (Brun, 1987) and MCNP (Briesmeister, 1993) codes (Masarik & Beer, 1999). The main nuclear reactions leading to cosmogenic ^{81}Kr are proton- and neutron-induced spallation of the stable nuclides ^{82}Kr, ^{83}Kr, ^{84}Kr, and ^{86}Kr, as well as nuclear reactions ^{80}Kr(n,γ) ^{81}Kr and ^{82}Kr(γ, n)^{81}Kr. The cross sections for spallation reactions were evaluated in earlier calculations (Masarik & Beer, 1999). The cross sections for the (n,γ) and (γ,n) reactions are taken from the ENDF-VI/b library linked to the MCNP code.

The primary cosmic-ray flux at the Earth's orbit has two components: galactic (GCR) and solar (SCR). The GCR particles are a mixture of ~87% protons, ~12% α particles, and ~1% heavier nuclei (Simpson, 1983). The energy distributions of all nuclei are quite similar if compared in terms of energy per nucleon. The analytical formula for the differential spectra of GCR primary protons is expressed as (Castagnoli & Lal, 1980; Simpson, 1983)

$$J(E_p,\phi) = C_p \frac{E_p(E_p+2m_p)(E_p+x+\phi)^{-2.65}}{(E_p+\phi)(E_p+2m_p+\phi)} \tag{2}$$

Here E_p (MeV) is the kinetic energy of the proton, m_p (MeV) is the rest mass, ϕ (MeV) is the parameter describing the modulation effect of the solar activity, $C_p = 1.24 \times 10^6$ cm^{-2} s^{-1} MeV^{-1} is the normalization coefficient, and $x = 780 \exp(-2.5 \times 10^{-4} E_p)$ MeV. For α particles and heavier nuclei in GCR, there are corresponding formulae with parameters of slightly different values (Lal, 1988). Within the Earth's magnetic field, α particles are simulated separately from the protons because of the different geomagnetic effects on these two nuclides. Fits to lunar experimental data (Masarik & Reedy, 1994) indicate that the effective flux of protons and α particles with energies above 10 MeV per nucleon at 1 A.U. is 4.56 nucleons cm^{-2} s^{-1}. This value corresponds to the long-term average of $\phi = 550$ MeV for the modulation parameter (Reedy, 1987)

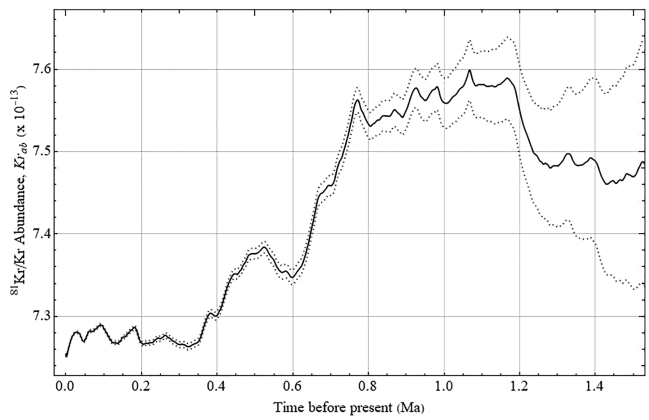

Figure 1. The isotopic abundance of ^{81}Kr in the atmosphere calculated over the past 1.5 Ma. The middle curve (solid) uses a constant production rate of P(2 Ma) for $time_{BP}$ >2 Ma. The top and bottom (dotted) curves represent production rates two standard deviations (taken from the full range of production rates from 0 to 2 Ma) higher and lower than P(2), respectively, for $time_{BP}$ > 2 Ma.

The SCR particles consisting of ~98% protons and ~2% heavier nuclei (Simpson, 1983), with energies in the range of 1–100 MeV, can be neglected. Because of their relatively lower energies, nuclear reactions in the Earth's atmosphere are limited to high geomagnetic latitudes and the very top of the atmosphere. Previous calculations showed that, for cosmogenic nuclides produced in spallation, the contribution from SCR is below 1% (Masarik & Beer, 1999). This percentage can increase by a factor of a few, but only at high latitudes and during strong solar events.

Based on the relative geomagnetic field intensities recorded over the past 2 Myr (Valet et al., 2005), we calculate the atmospheric ^{81}Kr/Kr abundance, $Kr_{ab,}$ at a given time before present in Ma, $time_{BP}$, by integrating the production rate $P(t)$ from equations (1) and (2) weighted by the ^{81}Kr decay factor

$$Kr_{ab}(time_{BP}) = \int_{time_{BP}}^{T} P(t)\cdot 2^{-\frac{t-time_{BP}}{t_{1/2}}} dt \tag{3}$$

In order to obtain an estimated range for the unknown initial value of Kr_{ab} at 2 Ma, we integrate from $time_{BP}$ to T = 4 Ma in 1-kyr intervals. For $time_{BP}$ beyond 2 Ma, where we lack magnetic field data to calculate a production rate, we have assumed constant production rates of P(2 Ma), P(2 Ma) − s, and P(2 Ma) + s, to generate the three curves shown in Figure 1, where s is 2 standard deviations of the range of production rates at t < 2 Ma. Independent of the initial value, the calculation provides consistent results from present to approximately 1.5 Ma within the uncertainty range indicated by the two outer curves.

Using equation (3), the present day Kr_{ab} is determined to be $(7.3 \pm 1.8) \times 10^{-13}$ (all uncertainties reported are 1σ). The error is dominated by the ~25% systematic uncertainties on the input parameters (e.g., cross sections, neutron fluxes) of the production rate. A more detailed discussion on the uncertainties in similar analyses is given in Masarik et al. (2001). Although the standard deviations of the stacked paleomagnetic field records are on the order of 15–20% (Frank et al., 1997; Valet et al., 2005), short-term variations of such amplitudes around the adopted smoothed field intensity curves have a negligible influence on the integrated production rates of ^{81}Kr. Therefore, only the systematic errors in the paleomagnetic records significantly contribute to the uncertainty of the production rate.

3. Measurement of the Atmospheric ^{81}Kr/Kr Isotopic Abundance

The atmospheric ^{81}Kr/Kr ratio has previously been measured a few times using the Low-Level Decay Counting (LLC) method (Barabanov & Pomansky, 1975; Kuzminov & Pomansky, 1980; Loosli & Oeschger, 1969), with results varying by as much as a factor of 2 (see Table 1). The main difficulties for LLC lie in the extremely low counting rate and the need to understand and calibrate the counting efficiency and background of the detector. The ^{81}Kr/Kr ratio has also been measured once using the Accelerator Mass Spectrometry method (Collon et al., 1997; Collon et al., 1999). However, the Accelerator Mass Spectrometry measurement had relatively large statistical uncertainty (~20%) and possibly undetermined systematic uncertainties.

Table 1
Measurements of the ^{81}Kr Decay Activity and the ^{81}Kr/Kr Isotopic Abundance in the Atmosphere

Reference	Method	^{81}Kr activity (dpm/L_{Kr})	^{81}Kr/Kr abundance
Loosli and Oeschger (1969)	LLC	**0.100 ± 0.010**	$(6.6 \pm 0.7) \times 10^{-13}$
Barabanov and Pomansky (1975)	LLC	**0.046 ± 0.010**	$(3.0 \pm 0.7) \times 10^{-13}$
Kuzminov and Pomansky (1980)	LLC	**0.067 ± 0.003**	$(4.4 \pm 0.2) \times 10^{-13}$
Collon et al. (1997)	AMS	0.081 ± 0.019	$\mathbf{(5.3 \pm 1.2) \times 10^{-13}}$
This work (2019)	ATTA/MS/dilution	0.138 ± 0.005	$\mathbf{(9.3 \pm 0.3) \times 10^{-13}}$
This work (2019)	Calculation	0.11 ± 0.03	$(7.3 \pm 1.8) \times 10^{-13}$

Note. The values in bold, measured directly, are used to derive the corresponding values in plain text. ^{81}Kr decay activity is in units of decays per minute per liter of Kr gas at STP.

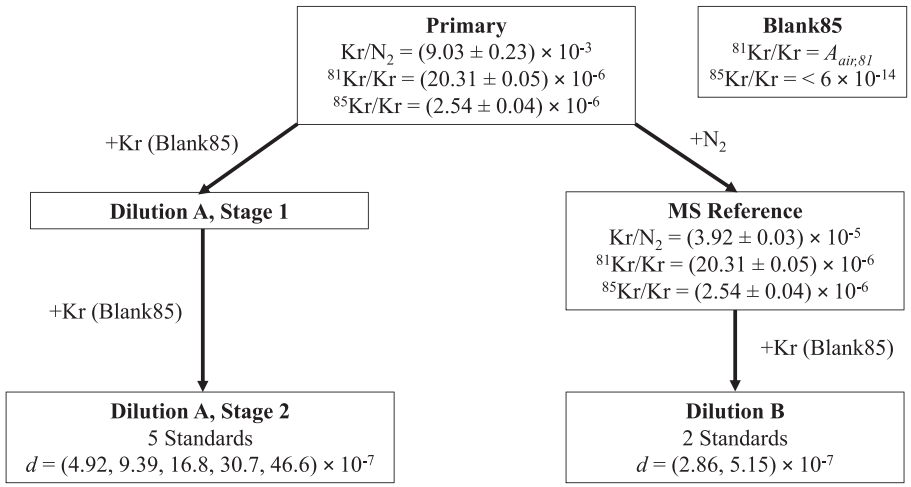

Figure 2. Details of Blank85, Primary, MS Reference, and Standard samples. A diagram of the two dilution processes A and B, including the respective Kr/N_2, $^{81}Kr/Kr$, and $^{85}Kr/Kr$ ratios of the Primary and MS Reference gases measured by mass spectrometry, and the dilution factors d of the Standards (see supporting information for further details on mass spectrometry measurements and dilution processes).

Since the advent of ATTA-3 (Jiang et al., 2012), a new atom-counting instrument based on the Atom Trap Trace Analysis method, measuring $^{81}Kr/Kr$ ratios in environmental samples, has become routine and ^{81}Kr dating of old groundwater and ice samples is now available to the Earth science community at large (Lu et al., 2014). An ATTA-3 instrument can be used to selectively trap atoms of the radioactive isotopes ^{81}Kr or ^{85}Kr in the isotopic abundance range of 10^{-14}–10^{-10}, as well as the stable isotopes (Jiang et al., 2012). In particular, ^{83}Kr (stable, isotopic abundance = 11.5%) is trapped for normalization in isotope-ratio measurements. While the abundance of each isotope is proportional to its trap capture rate, the proportionality coefficient for each isotope depends on the details of the trap instrument and cannot be derived a priori. For isotope dating, the coefficients need to be kept stable from one measurement to another, but their values need not be determined because they cancel in the ratio-of-isotope-ratio calculation between the isotope ratios of the sample and the atmosphere. However, for the purpose of this work, in order to derive the $^{81}Kr/Kr$ isotopic abundance of the atmosphere, we must first calibrate the ATTA-3 instrument with a set of standard samples whose isotope ratios are known independently.

The set of ^{81}Kr *Standard* samples were derived from an enriched *Primary* sample of krypton gas with a $^{81}Kr/Kr$ ratio ($A_{prim,81}$) on the order of 10^{-5} and a $^{85}Kr/Kr$ ratio ($A_{prim,85}$) on the order of 10^{-6}. The Primary sample is a mixture of accelerator-produced ^{81}Kr contained in a N_2 carrier gas and reactor-produced ^{85}Kr in an atmospheric krypton gas. At this highly enriched level, $A_{prim,81}$ and $A_{prim,85}$ can both be precisely determined using noble-gas mass spectrometry and were measured to be 20.31 ± 0.05 and 2.54 ± 0.04 ppm, respectively. Details of the Primary and Standard samples are shown in Figure 2.

This enriched Primary sample was then precisely diluted using *Blank85*, a krypton gas sample extracted from the atmosphere in 1944 (Kuzminov & Pomansky, 1980). LLC shows the $^{85}Kr/Kr$ ratio of this krypton gas to be below the detection limit of 6×10^{-14}, and ATTA measurements show the $^{81}Kr/Kr$ ratio of Blank85 to be within 1% of the modern atmospheric value (by a relative comparison, as used in age dating). This $^{81}Kr/Kr$ measurement allows us to treat the $^{81}Kr/Kr$ abundance of Blank85 as the modern atmospheric value. At the same time, it also demonstrates that the modern $^{81}Kr/Kr$ abundance has no significant anthropogenic contributions. Various levels of dilution by about 5–6 orders of magnitude were performed to lower the $^{81}Kr/Kr$ and $^{85}Kr/Kr$ ratios to levels within the measurement range of ATTA. The resulting Standards thus have isotopic ratios A_{stan} of

$$A_{stan,81} = A_{air,81} + d \cdot A_{prim,81} \tag{4}$$

$$A_{stan,85} = d \cdot A_{prim,85} \tag{5}$$

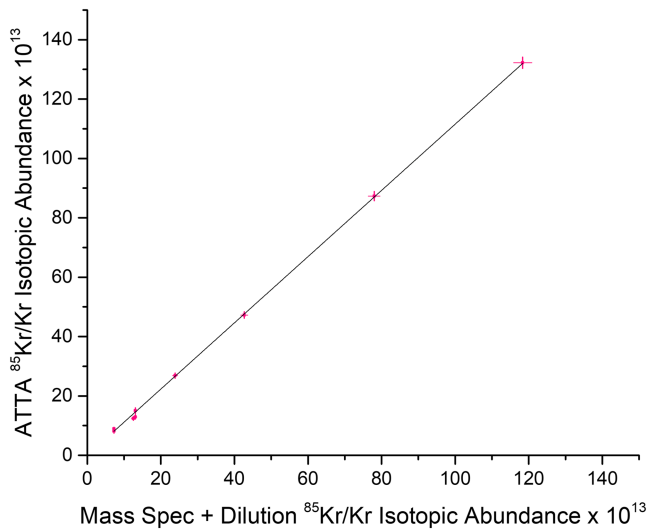

Figure 3.. The ^{85}Kr Standard comparison. The ^{85}Kr isotopic abundances measured with ATTA calibrated using LLC versus ^{85}Kr isotopic abundances expected in the Standards from mass spectrometry and precision dilution, all adjusted to 1 August 2018. The black line represents a linear fit forced through the origin with a slope of 1.115 ± 0.014 and a reduced χ^2 value of 1.7. There is an additional systematic uncertainty of ±0.028 on the slope due to uncertainties in dilution (see supporting information), which accounts for the excess reduced χ^2 value above unity.

where d (~10^{-5}–10^{-6}, $1-d \approx 1$) is the fraction of krypton gas from the Primary sample in the Standard and $A_{air,81}$ is the modern atmospheric ^{81}Kr/Kr ratio that we aim to determine in this work.

In the ATTA-3 apparatus, atoms of a targeted isotope (^{81}Kr, ^{85}Kr, or the control isotope ^{83}Kr) are captured by resonant laser light into a trap. For the rare isotopes ^{81}Kr and ^{85}Kr, the trapped atoms are counted individually by observing their fluorescence, and their capture rates (R_{81} and R_{85}) are recorded. In addition to trapping these two radioactive isotopes, ATTA-3 is also used to trap and measure the loading rate (R_{83}) of the stable isotope ^{83}Kr for normalization (Jiang et al., 2012; Jiang et al., 2014) The ratio R_{81}/R_{83} is proportional to the isotopic abundance A_{81}. The ATTA-3 apparatus has demonstrated the ability to measure this ratio with 1% precision, given sufficient atom counting statistics (Zappala et al., 2017).

For each of the Standard samples, the ratios $(R_{81}/R_{83})_{stan}$ and $(R_{85}/R_{83})_{stan}$ are measured with ATTA. The values are then compared to those of a dedicated lab reference sample, $(R_{81}/R_{83})_{ref}$ and $(R_{85}/R_{83})_{ref}$, to generate the fractional reference values (fR) of the standard sample defined as

$$fR_{stan,81} = \left(\frac{R_{81}}{R_{83}}\right)_{stan} \Big/ \left(\frac{R_{81}}{R_{83}}\right)_{ref} = 1 + d\cdot\frac{A_{prim,81}}{A_{air,81}} \tag{6}$$

$$fR_{stan,85} = \left(\frac{R_{85}}{R_{83}}\right)_{stan} \Big/ \left(\frac{R_{85}}{R_{83}}\right)_{ref} = d\cdot\frac{A_{prim,85}}{A_{ref,85}} \tag{7}$$

These relations are derived from equations (3) and (4), given that the ^{81}Kr/Kr ratio of the reference gas is identical to that of the air ($A_{ref,81} = A_{air,81}$); d is determined in the precision dilution procedure.

As a consistency check for the method, $fR_{stan,85}$ measured with ATTA are converted to isotopic abundances and plotted in Figure 3 against the abundances taken from the results of mass spectrometry and precision dilution. For ^{85}Kr, ATTA is calibrated to LLC in order to determine the isotopic abundances. The uncertainty on this calibration is primarily due to a ^{85}Kr reference standard created in 1986, which was measured by differential counting with an error of ~10%, typical at the time. This error affects the overall slope of the fit, but not the linearity of the data. The resulting slope is 1.115 ± 0.028 (systematic) ± 0.014 (statistical). The systematic error is the result of a common 3% error in the dilution of five of the seven Standards shown (see supporting information). These data confirm the linearity of the dilution process and analysis method to be at the 1.8% level. The deviation of the slope from unity is expected within the uncertainty of the LLC calibration of ATTA. We note that this deviation has no direct impact on the following ^{81}Kr measurement.

To extract $A_{air,81}$, equation (6) is rearranged as

$$d\cdot\left(A_{prim,81}\right) = A_{air,81}\left(fR_{stan,81} - 1\right) \tag{8}$$

in order to relate the results of ATTA measurements (represented on the right side of the equation) against the results from mass spectroscopy and dilution (represented on the left) such that the slope of a linear regression will be $A_{air,81}$. This plot is shown in Figure 4 and yields a value for $A_{air,81}$ of 9.30 ± 0.18 (systematic) ± 0.07 (statistical) × 10^{-13}. The systematic uncertainty is dominated by the dilution process (see supporting information). The statistical uncertainty is limited by the dilution precision and the ATTA measurements. In this experiment the relative ATTA uncertainties (1–3% for each individual measurement) are significantly lower than is typically seen in environmental samples (3–4% for an individual measurement) because the enrichment of the samples well above the modern atmospheric value provides, respectively, higher atom counting statistics. In comparison, the statistical uncertainties from the mass spectrometry measurements are negligible. As shown in Table 1, our new value of $A_{air,81}$ is significantly higher than previous results.

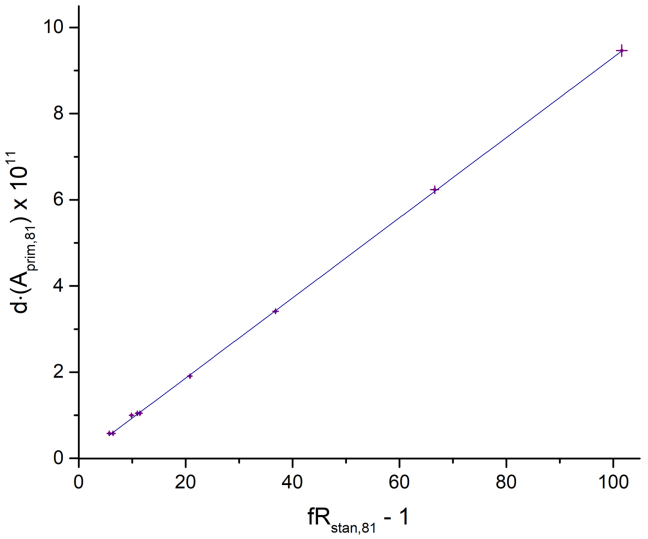

Figure 4. Measured ^{81}Kr atmospheric abundance. The dilution factor d times $A_{prim,81}$ rescaled by 10^{11} versus ($fR_{stan,81} - 1$) measured by ATTA. The blue line represents a linear fit (equation (8)) forced through the origin with a slope of 9.30 ± 0.07 and a reduced χ^2 value of 1.3. There is an additional systematic uncertainty of ±0.018 on the slope due to the dilution procedure (see supporting information), which accounts for the excess in the reduced χ^2 value above unity.

The measured ^{81}Kr/Kr abundance agrees with the theoretically derived value in this work, demonstrating the validity of the cosmic-ray flux model and its input parameters. However, due to the relatively large 25% model uncertainty the theoretical value also agrees with two of the previous experimental results on the lower abundance side. As such, the experimental uncertainty of ~3% for ^{81}Kr/Kr achieved in this work should motivate investigations into improving the accuracy of the theoretical models.

The results of this work will have broad implications beyond the understanding of cosmic rays. As noted, the dominant error in the production model is an overall systematic scaling factor, and thus, the relative variation of the production is much better understood. As such, by pinning the model to the newly measured present-day ^{81}Kr/Kr value of this work, a precise input function can be extrapolated up to 1.5 Ma for this isotope. Such an input function is critical to the rapidly growing and improving field of radiokrypton dating, particularly in applications like paleoclimate studies (Buizert et al., 2014; Yokochi et al., 2019) where absolute ages are of great importance. The historical atmospheric ^{81}Kr abundance derived here is found to be in good agreement with previous estimations of its relative variations (Buizert et al., 2014). An additional and independent outcome of this work is the production of a well-characterized ^{85}Kr standard sample that will aid in future recalibration of LLC instrumentation.

Acknowledgments
This work and the TRACER Center at Argonne National Laboratory is supported by the Department of Energy, Office of Nuclear Physics, under contract DE-AC02-06CH11357. W.J., Z.T.L., and part of the work were supported by the National Natural Science Foundation of China (41727901) and the National Key Research and Development Program of China (2016YFA0302200). B.M.K. was supported by the Director, Office of Science, Office of Basic Energy Sciences, Division of Chemical Sciences, Geosciences, and Biosciences, of the U.S. Department of Energy under contract DE-AC02-05CH11231. Noble gas mass spectrometry measurements were conducted at LLNL under contract DE-AC52-07NA27344. The authors declare no competing interests. The data supporting the findings of this study are available at Zappala et al. (2020), Replication data for "Atmospheric ^{81}Kr as an integrator of cosmic-ray flux on the hundred-thousand-year time scale," https://doi.org/10.7910/DVN/7AJLJM, Harvard Dataverse, and within the references.

References

Baglin, C. M. (2008). Nuclear data sheets for A = 81. *Nucl. Data Sheets*, *109*, 2257–2437. https://doi.org/10.1016/j.nds.2008.09.001

Barabanov, I. R., & Pomansky, A. A. (1975). Atmospheric abundance of ^{81}Kr and cosmic ray intensity. *Proceedings of the International Conference on Low-Radioactivity Measurements and Applications*, The High Tatras, Czechoslovakia, 405-408.

Bard, E., & Frank, M. (2006). Climate change and solar variability: What's new under the Sun? *Earth Planet. Science Letters*, *248*, 1–14. https://doi.org/10.1016/j.epsl.2006.06.016

Baumgartner, S., Beer, J., Masarik, J., Wagner, G., Meynadier, L., & Synal, H.-A. (1998). Geomagnetic modulation of the ^{36}Cl flux in the GRIP ice core, Greenland. *Science*, *279*(5355), 1330–1332. https://doi.org/10.1126/science.279.5355.1330

Beer, J., Blinov, A. V., Bonani, G., Hofmann, H. J., Finkel, R., Lehmann, B., et al. (1990). Use of ^{10}Be in polar ice to trace the 11-year cycle of solar activity. *Nature*, *347*(6289), 164–166. https://doi.org/10.1038/347164a0

Beer, J., McCracken, K. G., Abreu, J., Heikkila, U., & Steinhilber, F. (2013). Cosmogenic radionuclides as an extension of the neutron monitor era into the past: Potential and limitations. *Space Science Reviews*, *176*, 89–100.

Beer, J., McCracken, K. G., & von Steiger, R. (2011). *Cosmogenic radionuclides: Theory and applications in the terrestrial and space environments*. Berlin, Germany: Springer.

Briesmeister, J. F. (1993). *MCNP: A general Monte Carlo N-particle transport code version 4A, LA-12625-M*. LANL Los Alamos, USA: Los Alamos National Laboratory.

Brun, B. (1987). *GEANT3 user's guide*, Rep. In *DD/EE/84-1 Geneva*. Switzerland: European Organization for Nuclear Research.

Buizert, C., Baggenstos, D., Jiang, W., Purtschert, R., Petrenko, V. V., Lu, Z.-T., Müller P, et al. (2014). Radiometric ^{81}Kr dating identifies 120,000-year-old ice at Taylor Glacier, Antarctica. *Proceedings of the National Academy of Sciences 111*, 6876-6881.

Carcaillet, J. T., Thouveny, N., & Bourles, D. L. (2003). Geomagnetic moment instability between 0.6 and 1.3 Ma from cosmonuclide evidence. *Geophysical Research Letters*, *30*, 1792. https://doi.org/10.1029/2003GL017550

Castagnoli, G., & Lal, D. (1980). Solar modulation effects in terrestrial production of carbon-14. *Radiocarbon*, *22*, 133–158.

Chen, C.-Y., Li, Y. M., Bailey, K., O'Connor, T. P., Young, L., & Lu, Z.-T. (1999). Ultrasensitive isotope trace analysis with a magneto-optical trap. *Science*, *286*(5442), 1139–1141. https://doi.org/10.1126/science.286.5442.1139

Collon, P., Antaya, T., Davids, B., Fauerbach, M., Harkewicz, R., Hellstrom, M., et al. (1997). Measurement of ^{81}Kr in the atmosphere. *Nucl. Instrum. Meth. B*, *123*(1-4), 122–127. https://doi.org/10.1016/S0168-583X(96)00674-X

Collon, P., Cole, D., Davids, B., Fauerbachs, M., Harkewicz, R., Kutschera, W., et al. (1999). Measurement of the long-lived radionuclide ^{81}Kr in pre-nuclear and present-day atmospheric krypton. *Radiochimica Acta*, *85*, 13–19.

Finkel, R. C., & Nishiizumi, K. (1997). Beryllium 10 concentrations in the Greenland Ice Sheet Project 2 ice core from 3–40 ka. *Journal of Geophysical Research, Oceans*, *102*(26), 699–26,706. https://doi.org/10.1029/97JC01282

Frank, M., Schwarz, B., Baumann, S., Kubik, P. W., Suter, M., & Mangini, A. (1997). A 200 kyr record of cosmogenic radionuclide production rate and geomagnetic field intensity from ^{10}Be in globally stacked deep-sea sediments. *Earth and Planetary Science Letters*, *149*, 121–129.

Heikkila, U., Beer, J., Abreu, J., & Steinhilber, F. (2013). On the atmospheric transport and deposition of the cosmogenic radionuclides (^{10}Be): A review. *Space Science Reviews*, *176*, 321–332.

Jiang, W., Bailey, K., Lu, Z.-T., Mueller, P., O'Connor, T. P., Cheng, C.-F., et al. (2012). An atom counter for measuring ^{81}Kr and ^{85}Kr in environmental samples. *Geochimica et Cosmochimica Acta*, *91*, 1–6. https://doi.org/10.1016/j.gca.2012.05.019

Jiang, W., Bailey, K., Lu, Z.-T., Mueller, P., O'Connor, T. P., & Purtschert, R. (2014). Ion current as a precise measure of the loading rate of a magneto-optical trap. *Optics Letters*, *39*(2), 409–412. https://doi.org/10.1364/OL.39.000409

Kuzminov, V. V., & Pomansky, A. A. (1980). New measurment of the ^{81}Kr atmospheric abundance. *Radiocarbon*, *22*, 311–317.
Lal, D. (1988). Theoretically expected variations in the terrestrial cosmic-ray production of isotopes. In G. C. Castagnoli (Ed.), *Solar-Terrestrial Relationships* (pp. 216–233). Society Italiana di Fisica: Bologna, Italy.
Loosli, H., & Oeschger, H. (1969). ^{37}Ar and ^{81}Kr in the atmosphere. *Earth and Planetary Science Letters*, *7*, 67–71.
Lu, Z.-T., Schlosser, P., Smethie, W. M. Jr., Sturchio, N. C., Fischer, T. P., Kennedy, B. M., et al. (2014). Tracer applications of noble gas radionuclides in the geosciences. *Earth-Science Reviews*, *138*, 196–214. https://doi.org/10.1016/j.earscirev.2013.09.002
Masarik, J., & Beer, J. (1999). Simulation of particle fluxes and cosmogenic nuclides production in the Earth's atmosphere. *Journal of Geophysical Research*, *104*, 12,099–12,111. https://doi.org/10.1029/1998JD200091
Masarik, J., Frank, M., Schafer, J. M., & Wieler, R. (2001). Correction of in situ cosmogenic nuclide production rates for geomagnetic field intensity variations during the past 800,000 years. *Geochimica et Cosmochimica Acta*, *65*, 2995–3003.
Masarik, J., & Reedy, R. C. (1994). Effects of bulk chemical composition on nuclide production processes in meteorites. *Geochimica et Cosmochimica Acta*, *58*, 5307–5317.
McCracken, K. G., Beer, J., & McDonald, F. B. (2002). A five-year variability in the modulation of the galactic cosmic radiation over epochs of low solar activity. *Geophysical Research Letters*, *29*, 2161. https://doi.org/10.1029/2002GL015786
Ozima, M., & Podosek, F. A. (2001). *Noble Gas Geochemistry* (2nd ed.). Cambridge, United Kingdom: Cambridge University Press.
Reedy, R. C. (1987). Nuclide production by primary-ray protons, Proceedings of the 17th Lunar Planetary Science Conference. *Journal of Geophysical Research*, *92*, 697–702.
Sharma, M. (2002). Variation in solar magnetic activity during the last 200,000 years: Is there a Sun climate connection? *Earth and Planetary Science Letters*, *199*, 459–472.
Simpson, J. A. (1983). Elemental and isotopic composition of the galactic cosmic rays. *Annual Review of Nuclear and Particle Science*, *33*, 323–381.
Usoskin, I. G., & Kovaltsov, G. A. (2008). Production of cosmogenic ^{7}Be isotope in the atmosphere: Full 3D modeling. *Journal of Geophysical Research*, *113*, D12107. https://doi.org/10.1029/2007JD009725
Valet, J.-P., Meynadier, L., & Guyodo, Y. (2005). Geomagnetic dipole strength and reversal rate over the past two million years. *Nature*, *435*, 802–805. https://doi.org/10.1038/nature03674
Webber, W., & Higbie, P. (2003). Production of cosmogenic Be nuclei in the Earth's atmosphere by cosmic rays: Its dependence on solar modulation and the interstellar cosmic ray spectrum. *Journal of Geophysical Research*, *108*, 1355. https://doi.org/10.1029/2003JA009863
Yokochi, R., Ram, R., Zappala, J. C., Jiang, W., Adar, E., Bernier, R., et al. (2019). Radiokrypton unveils dual moisture sources of a deep desert aquifer. *Proceedings of the National Academy of Sciences*, *116*(33), 16222–16227. https://doi.org/10.1073/pnas.1904260116
Zappala, J. C., Bailey, K., Mueller, P., O'Connor, T. P., & Purtschert, R. (2017). Rapid processing of ^{85}Kr/Kr ratios using Atom Trap Trace Analysis. *Water Resources Research*, *53*, 2553–2558. https://doi.org/10.1002/2016WR020082

References From the Supporting Information

Bereiter, B., Kawamura, K., & Severinghaus, J. P. (2018). New methods for measuring atmospheric heavy noble gas isotope and elemental ratios in ice core samples. *Rapid Communications in Mass Spectrometry*, *32*(10), 801–814. https://doi.org/10.1002/rcm.8099
Brendel, K. J., Kuipers, J., Barkema, G. T., & Hoyng, P. (2007). An analysis of the fluctuations of the geomagnetic dipole. *Phys. Earth Planet. Interiors*, *162*, 249–255.
Champion, K. S. W., Cole, A. E., & Kantor, A. J. (1985). Standard and reference atmosphere. In A. S. Jursa (Ed.), *Handbook of Geophysics and the Space Environment*. U.S. Air Force, USA: Air Force Geophys. Lab.
Clark, J. F., Davisson, M. L., Hudson, G. B., & Macfarlane, P. A. (1998). Noble gases, stable isotopes, and radiocarbon as tracers of flow in the Dakota aquifer, Colorado and Kansas. *Journal of Hydrology*, *211*, 151–167.
Gosse, J. C., Reedy, R. C., Harrington, C. D., & Poths, J. (1996). Overview of the workshop on secular variations in production rates of cosmogenic nuclides on Earth. *Radiocarbon*, *38*, 135–147.
Masarik, J., & Beer, J. (2009). An updated simulation of particle fluxes and cosmogenic nuclide production in the Earth's atmosphere. *Journal of Geophysical Research*, *114*, D11103. https://doi.org/10.1029/2008JD010557
Masarik, J., & Reedy, R. C. (1995). Terrestrial cosmogenic-nuclide production systematic calculated from numerical simulations. *Earth and Planetary Science Letters*, *136*, 381–395.
Nobuyuki, A., & Makide, Y. (2005). The concentration of krypton in the atmosphere: Its revision after half a century. *Chemistry Letters*, *34*, 1396–1397.
Shea, M. A., & Smart, D. F. (1992). Recent and historical solar proton events. *Radiocarbon*, *34*, 255–262.
Surano, K. A., Hudson, G. B., Failor, R. A., Sims, J. M., Holland, R. C., MacLean, S. C., & Garrison, J. C. (1992). Helium-3 mass spectrometry for low-level tritium analysis of environmental samples. *Journal of Radioanalytical and Nuclear Chemistry*, *161*, 443–453.
Tauxe, L. (1985). Sedimentary records of relative paleointensity of the geomagnetic field: Theory and practice. *Reviews of Geophysics*, *31*, 319–354.
Visser, A., Moran, J. E., Hillegonds, D., Singleton, M. J., Kulongoski, J. T., Belitz, K., & Esser, B. K. (2016). Geostatistical analysis of tritium, groundwater age and other noble gas derived parameters in California. *Water Research*, *91*, 314–330. https://doi.org/10.1016/j.watres.2016.01.004
Wagner, G., Masarik, J., Beer, J., Baumgartner, S., Imboden, D., Kubik, P. W., et al. (2000). Reconstruction of the geomagnetic field between 20 and 60 kyr BP from cosmogenic radionuclides in the GRIP ice core. *Nuclear Instruments and Methods in Physics Research B*, *172*(1-4), 597–604. https://doi.org/10.1016/S0168-583X(00)00285-8